A late Holocene molluscan-based palaeoenvironmental reconstruction from southern Mesopotamia: implications for the palaeogeographic evolution of the Arabo-Persian Gulf

Ismael D.S. Al-Ameri[1, 2, *], Rebecca M. Briant[2]

[1] Department of Geography, Ibn Rushd, University of Baghdad, Bab Al-Muadham Campus, Iraq
[2] Department of Geography, Birkbeck, University of London, Malet Street, London, WC1E 7HX, UK

Abstract

This study provides important tie-point sequences that allow better constraint on the timing and position of the marine transgression of the Arabo-Persian Gulf in southern Mesopotamia east of the ancient site of Ur in Iraq. The Mesopotamian civilisation contains the oldest city states known in the world and many other significant archaeological sites. It remains, however, an open question about the nature of the water resources that were available to these civilisations. Whilst the most northerly extent of the Arabo-Persian Gulf has been dated to ca. 6000 BP, it is much less clear how quickly the deltas of the Tigris, Euphrates and Karun infilled what is now the southern Mesopotamian Plain. Specifically, the position of the coastline is unclear at ca. 5000 BP when key city states such as Ur were founded, and also ca. 3000 BP at the start of the dynastic period, with various authors differing strongly. This is important to uncover because human populations are strongly dependent on water resources, both freshwater for drinking and washing, and freshwater and marine for naturally-occurring sources of protein from fish and wildfowl. This study addresses these concerns by the study of two sedimentary cores from locations further north than any previous studies. We have undertaken the first ever detailed molluscan analysis from such sequences in this region. This is combined with four radiocarbon dates and some indication of pollen abundance from a very sparse assemblage. Results from our study suggest that the coastline was further north than previously suggested at ca. 3000 BP, with rapid regression after this time.

Keywords: Mesopotamia, Holocene, Radiocarbon age, Palaeoclimate, Mollusca.

1.1 Introduction

Mesopotamia has long been seen as the cradle of civilisation, a civilisation that did not derive from a prior one but appeared and developed since prehistoric times (Baqer, 1980). Between 8000–5500 BP, human populations increased and aggregated into small towns and nucleated villages during the Ubaid period and earlier (Ur, 2014, Table 1). These communities ultimately provided the foundation for the integrated state-level societies and urban centres that developed by 5000 BP, during the Uruk period. During the Uruk period social complexity and resource consumption accelerated (Clarke, et al., 2016), with technological innovations including large-scale irrigation, agriculture and writing (Kennett and Kennett, 2006). Kennett and Kennett (2006) argue that the initial development of settled city states was strongly linked to coastal and aquatic habitats, with water resources being crucial to provide freshwater, food, small-scale irrigation and efficient transport of people and goods for trade. They further discuss that aridification and a slowdown in marine transgression around 6-5000 BP led to a concentration of more people in a smaller area with fewer resources. This created the potential for conflict, requiring the development of larger population centres for more effective use of irrigation technology as well as defensive purposes. The early Holocene marine transgression is clearly linked to the position of key archaeological sites at this time (e.g. Cooke, 1987; Sanlaville, 1989).

Following the first establishment of these cities ca. 5000 BP, the Sumerian civilisation flourished until ca. 3700 BP, when populations declined, with the final transition to the Assyrian Empire around 3000

BP (Ur, 2012; 2014, Table 1). The cause of this population decline is as yet unclear, although some researchers suggest that it may have been linked to an aridification event around 4200 BP (e.g. Dixit et al., 2014). From ca. 5000-1000 BP, it is much less clear how the archaeological sites relate spatially to the development of the coastline (cf. Naval Intelligence Division, 1944; Aqrawi, 2001; Hritz et al., 2012; Table 1). These conflicting suggestions are based on contrasting data sources. The Naval Intelligence Division (1944) have a starting point that the coastline was near to key Sumerian cities at ca. 5000 BP. Shoreline progradation was then gradually modelled due to deposition within both the Tigris-Euphrates and Karun Deltas based on measurements of sedimentation rates within these systems in the 1940s. They suggested that rapid progradation of the Karun delta (also noted in historical texts) blocked direct marine influence upstream of Basra ca. 2000 BP when the delta reached the western edge of the Mesopotamian basin, and that further progradation caused the present-day shoreline position to be reached ca. 1000 BP. In contrast, Aqrawi (2001) suggested that progradation occurred more rapidly, with the present-day shoreline position reached 2000 years earlier at 3000 BP (1000 BC). Aqrawi's (2001) reconstruction is based on mineralogical analysis of borehole cross-sections using various methods (diffractometer, ICP-AES, calcimeter, elemental analyser – Aqrawi et al., 1994). Using these analyses, Aqrawi identified tidal depositional environments using the presence of magnesium and calcite. These were then used to estimate shoreline position, with some radiocarbon dating of organic rich sediments. Radiocarbon dates from both sediments and shells are also reported by other authors (Plaziat and Younis, 2005; Hritz et al., 2012a). Hritz et al. (2012b) suggest a slightly different history of shoreline regression with a rate of transgression intermediate between the two other reconstructions. This reconstruction was based on detailed analysis of both previous datapoints and their own radiocarbon dated field observations (Hritz et al., 2012a). Their field observations comprised radiocarbon dates from archaeological sequences in the north of the Mesopotamian Plain on shell (Eridu – ca. 7500 - 4300 BP) and charcoal (Girhu – ca. 4500 BP) and sediment dates (all prior to ca. 6000 BP) from sequences retrieved near Basra. Cooke (1987) may also suggest an intermediate shoreline history, but the maps are too poorly drawn to state this for sure. A more detailed overview of changing historical perspectives on shoreline position in the Arabo-Persian Gulf may be found in Heyvaert and Baeteman (2007).

Delta, marsh and coast all provide distinct resources, and the balance between these environmental components in the landscape near to key Sumerian settlements is clearly important for the development of these civilisations. For this reason, the different shoreline histories proposed by these various authors are worthy of further investigation. Some of the differences in interpretation probably stem from the different data sources used, and still others from the difficulties in interpreting palaeoenvironments in the complex depositional environments within the estuarine-marine zone. There is also however a lack of environmental data from this region. In the present paper we have sampled two sedimentary cores from locations further north than previous studies to address the position of shoreline location. We report what are to our knowledge the first complete published and radiocarbon dated mollusc sequences from southern Mesopotamia. These allow us to better constrain the shoreline position and discuss the implications for the decline of the Sumerian civilisation. We suggest, in contrast to previous researchers, that the regression of the shoreline to its' present-day position occurred relatively late.

1.2 Geological setting

Mesopotamia is taken from the Greek and literally means "The land between two rivers." The rivers in this context are the Tigris and Euphrates, in the southern part of Iraq, between latitudes 29° 5' and 37° 22' N and longitudes 38° 45' and 48° 45' E. (Figure 1a). The alluvial plain in Iraq starts from Samarra and extends south-east to the Arabo-Persian Gulf, covering the fertile crescent between the Tigris and Euphrates rivers (Jassim and Goff, 2006). The two rivers meet at Qurna, where the tidal limit is located, and form the Shatt-al-Arab river which then drains into the Gulf (Figure 1b).

The Mesopotamian Plain is a large foreland basin of the Zagros Mountains to the north-east formed following collision of the Arabian and Eurasian Plates (Sharland et al., 2001). It slopes gently between Baghdad and Basra. Its elevation is ca. 150 m above sea level at highest and gradually decreases south and southwards to become ca. 35 m in Baghdad, 10–12 m in the central parts and 1–3 m in the south, within the Arabo-Persian Gulf area (Al-Jiburi and Al-Basrawi, 2011). In this low altitude section are the marshes of southern Iraq, one of the largest water bodies in the Middle East, confined to the triangular area between the cities of Amara to the north, Basra to the south and east and Nasiriya to the west (Figure 1b). The length of the area from north to south is approximately 200 km. The marshes are divided into three main areas: East Hammar, West Hammar and Central Marshes, from the latter two of which cores have been taken in this study (L1 and L2 on Figure 1b). Much of the area that was once under permanent or seasonal water was exposed by drainage activities in the 1990s (Hritz et al., 2012).

The fluvial systems of the Mesopotamian Plain drain into the Arabo-Persian Gulf. This feature is roughly 1,000 km long and ranges from 350 km to as little as 5 km wide at the Straits of Hormuz, where it joins the Gulf of Oman in the northern Indian Ocean. The Gulf is one of the shallowest inland seas in the world, with a mean depth of only 40 m and a maximum of 100 m near the Straits of Hormuz (Kennett and Kennett, 2006).

Location 1 (L1) of our study is in Central Marshes, in Dhi Qar and Maysan Governorates (Figure 1b). The geomorphological setting is on an island in the centre of the marsh, exposed following water level variation in the 1990s due to human modification of the Tigris-Euphrates system. The exact sample location was within a small (2-3 m wide) linear depression on the surface of the island at 31° 4' 3.2808 N, 47° 3' 16.4952 E. Central Marshes are at the heart of the Mesopotamian wetland ecosystem bounded by the Tigris river to the east and the Euphrates river in the south, covering an area of about 3,000 km^2. During flood periods this extends to well over 4,000 km^2 (UNEP, 2001).

Location 2 (L2) is in West Hammar Marsh in Dhi Qar Governorate (Figure 1b). The geomorphological setting is at the marsh margin, also exposed since the 1990s, at: 30° 56' 43.2522 N, 46° 53' 48.0732 E. West Hammar Marshes are situated almost entirely south of the Euphrates, extending from near Nasiriya in the west to the outskirts of Basra on the Shatt-al-Arab in the east. To the south, along their broad mud shoreline, the West Hammar Marshes are bordered by a sand dune belt of the southern desert. The marsh area ranges from 2,800 km^2 of contiguous permanent marsh and lake, extending to a total area of over 4,500 km^2 during periods of seasonal and temporary inundation (UNEP, 2001).

This study presents the sedimentary sequences, molluscan fossil data, and radiocarbon dating of four samples of mollusc shells from four depths to better constrain the timing and position of the shoreline of the Arabo-Persian Gulf in the southern region of Mesopotamia.

2. Materials and Methods

2.1 Sediment sequences

Sampling of the sediments described below was undertaken using a gouge auger, with retrieval of samples every 30 cm. Two sequences were retrieved from the locations described in section 1.2. The Central Marshes sequence (L1) is 5 m deep and samples were taken from 20, 50, 80, 110, 140, 170, 200, 230, 260, 290, 320, 350, 380, 410, 440, 470 and 500 cm depths (17 samples). The West Hammar Marshes sequence (L2) is 3.6 m deep and samples were taken from 30, 60, 90, 120, 150, 180, 210, 240, 270, 300, 330, and 360 cm depths (12 samples). Samples were stored refrigerated since they were collected. The initial sample was then subsampled for particle size analysis using a Malvern Mastersizer and wet sieved to retrieve multiple fossil groups as described in section 2.3.

2.2 Radiocarbon dating

Radiocarbon dating from sequences with marine influence can be problematic because of the marine reservoir effect (MRE) (e.g. Ascough et al., 2005). Marine organisms to be dated obtain their carbon from seawater that is very rarely in equilibrium with the atmosphere. This means that modern organisms may have an 'apparent age' and this effect needs to be corrected for when dating. However, the scale of the MRE is not consistent globally (e.g. Alves et al., 2018). This is because surface and deep water contain carbon of different ages (deep water being further out of equilibrium with the atmosphere) and exchange between the two occurs only in specific geographic areas. In addition, temperature affects the solubility of seawater, so atmospheric carbon dioxide is exchanged more effectively with surface water at lower temperatures (Alves et al., 2018). For these reasons, although there is a marine calibration curve for converting radiocarbon ages to calendar ages (Marine 13 – Reimer et al., 2013), local MRE corrections (ΔR) are also applied to reflect regional variations (Reimer and Reimer, 2016).

For the Arabo-Persian Gulf, there are two estimates of the MRE. The most recent is from Dohar in Qatar (Southon et al., 2002), from a bivalve shell of *Pinctada radiata* collected in 1952, yielding a ΔR of 163 ± 53 in Southon et al. (2002) and 180 ± 53 in the Marine Reservoir Database (Reimer and Reimer, 2016). An earlier ΔR value of 179 ± 66 was reported from coral in Al-Jurayd Island by Broecker et al. (1987), but not listed in the database. However, the sequences in this paper do not come from the Arabo-Persian Gulf. Instead they come from complex freshwater and estuarine marsh systems whose MRE has not been estimated. Local estimation of MRE is not possible because no collected pre-bomb shells exist because of decades of political instability within Iraq (Hritz et al., 2012a). For this reason, bulk sediment samples were not considered for radiocarbon dating because it was not clear what would be dated, and how much of the sediment would have been under marine influence. Instead, identified shell material was submitted. In the absence of sufficient mass of shell from terrestrial species, aquatic species were dated (Table 2). At Central Marshes (L1), there were sufficient freshwater shells of the special *Corbicula fluminalis* to submit these for dating and avoid the requirement to calculate the MRE. (The likelihood of a significant freshwater reservoir effect is small because of the significant depths of Quaternary sediment within the Mesopotamian plain overlying any limestone). At West Hammar Marshes (L2), the only sufficiently numerous shells were estuarine. An appropriate MRE for these is discussed in section 3.2.

All shell material was prepared for radiocarbon analysis at the Scottish Universities Environmental Research Centre (SUERC) by mechanical and ultrasonic cleaning before ca. 20% of the shell surface was removed using 1M HCl to eliminate any possible potential surface and edge contaminant $CaCO_3$, according to procedures listed in Dunbar et al. (2016). No tests were made to assess the likelihood of edge contamination, but this pretreatment was carried out in case such contamination had occurred.

2.3 Mollusc analysis

Samples sieved for mollusc analysis weighed approximately 250g before processing. These were wet sieved into 250μm, 500μm and 1mm fractions using tap water. Following sieving, samples were sorted and stored dry. All analysis used non-organic implements, ceramic dishes and glass storage tubes to avoid contamination with younger carbon. All samples from both sequences yielded fossil molluscs (Table 3), with freshwater, estuarine and marine affinities.

3. Results

3.1 Sedimentary sequence

The sedimentary sequences from both locations are very similar. In each case, they are dominated by silt (ca. 70-95%), with lower percentages of clay (ca. 5-25%) (Figures 2 and 3). The only level where sand is a significant percentage of the total is the highest sample from each sequence (Central Marsh, 20 cm depth sample – 10% sand; West Hammar Marsh, 30 cm depth sample – 13% sand).

In Central Marsh (L1, Figure 2), the uppermost 50 cm comprises light grey silty clay with varying shell content (more shell present from 20-50 cm depth). In the 50 cm sample only, silt percentages drop to 70% and clay rises to 25% (in the rest of the sequence silt comprises 80-95% and clay 3-18%). Gradationally underlying this, the sequence changes colour to a brown silty clay. The best shell preservation in this sequence occurs below ca. 250 cm (Figure 2).

At West Hammar Marsh (L2, Figure 3), the sequence is light grey in colour throughout. The uppermost 30 cm contains organic material in addition to shells, whereas below this, only shells are observed by eye. This is borne out by Figure 3, which shows similar good shell preservation throughout. In the 180 cm depth sample only, silt drops to 70% whilst clay rises to 25% (in the rest of the sequence silt comprises 80-90% and clay 5-13%).

3.2 Radiocarbon dating (Table 2)

In Central Marshes (L1), radiocarbon samples were taken from 320 and 500 cm depths. In both cases, the shell dated was the freshwater species *Corbicula fluminalis*. Date ranges for each were calibrated using OxCal 4 (Bronk Ramsay, 2009) and the IntCal13 calibration curve (Reimer et al., 2013). The sample from 320 cm (SUERC-74783 (GU44752)) had a radiocarbon age of 4159 ± 29 ^{14}C yr BP and a calibrated date range of ca. 4800 to 4500 cal. BP (Table 2). The sample from 500 cm (SUERC-74784 (GU44753)) had a radiocarbon age of 4578 ± 28 ^{14}C yr BP and a calibrated date range of 5500 to 5000 cal. BP. Given the significant change in molluscan assemblages between Zones 1 and 2, it is worth extrapolating these age estimates to provide an approximate age for the top of Zone 2 because there was insufficient shell material from 230 cm depth to date the top of this zone directly. Using a straight line fit between the median of the radiocarbon age at 320 cm and an assumed modern age (1950 AD) at the ground surface gives a rate of change (years/cm) of ca. 12.8 between 320 and 0 cm, and an estimated radiocarbon age for 230 cm depth of 2989 ± 149 ^{14}C yr BP (assuming a 5% error to account for errors in linear interpolation) and a calibrated age range using OxCal 4 (Bronk Ramsay, 2009) and IntCal13 (Reimer et al., 2013) of ca. 3500 to 20880 cal.BP.

In West Hammar Marsh (L2), a single shell of *Melanoides tuberculata* was dated from 180 cm and a single shell of *Melanopsis praemorsum* from 360 cm. Both of these species are freshwater and can also tolerate brackish conditions, although the more nodular form of *Melanopsis praemorsum* present suggests fresher water (section 3.3). Date ranges for each were calibrated using OxCal4 (Bronk Ramsay, 2009) and the Marine13 calibration curve (Reimer et al., 2013) Two regional marine offsets (ΔR) of 0 ± 50 years and 180 ± 63 years were applied to represent end members of possible marine reservoir effects within the estuarine system represented by this sequence (section 3.3). The ΔR value of 0 represents no marine influence and the ΔR of 180 represents the full marine influence of the Arabo-Persian Gulf (Southon et al., 2002; Reimer and Reimer, 2016). Hritz et al. (2012a) also radiocarbon dated *Melanoides tuberculata* and used a terrestrial calibration for their ages, arguing that as a short-lived filter feeder, this species would have been unaffected by any marine upwelling from deep water. They also argued that significant marine influence was unlikely because the sequences which they dated were interpreted as palustrine. In our study, the different values of ΔR used actually make very little difference to the final calibrated ranges. As a result, the full range of possible calibrated ages using both values of ΔR has been used in interpreting our sequence from West Hammar Marshes (L2).

The sample from 180 cm (SUERC-74778 (GU44750)) had a radiocarbon age of 2633 ± 29 BP and a calibrated date range of ca. 2500 to 2200 cal. BP (ΔR of 0) or 2400 to 2200 cal. BP (ΔR of 180). The sample from 360 cm (SUERC-74779 (GU44751)) had a radiocarbon age of 2111 ± 29 BP and a calibrated date range of ca. 1900 to 1600 cal. BP (ΔR of 0) or ca. 1800 to 1600 cal. BP (ΔR of 180). This radiocarbon age inversion could indicate reworking within the sequence, which is common within fluvial channel environments. Age inversion due to burrowing is also possible since these taxa live in soft bottom sediments (Plaziat and Younis, 2005). Thus the changes observed in palaeoenvironments from West Hammar Marsh can provide only a general picture of conditions over a wide time period compared to those from Central Marsh. Summing together the calibrated age ranges from both samples, this sequence comprises a reworked snapshot of the environment at West Hammar Marsh dating from ca. 2500 to 1600 cal. BP.

3.3 Mollusc sequence

The molluscs preserved in both sequences are predominantly aquatic, both marine and freshwater taxa, as well as those that tolerate brackish conditions, enabling the depositional environment to be interpreted in relation to Arabo-Persian Gulf coastline change in the past (cf. Langejans, et al., 2017). Shells also may be used to signal paleoenvironmental factors such as changes in climate and sea surface temperature and nearshore ecology (Ainis, et al., 2014). Identifications were made to the lowest taxonomic level for different habitats (marine, freshwater, and terrestrial molluscs) using multiple references. A total of 6 marine, 5 freshwater and 1 brackish taxa were observed in Central Marshes (L1, Figure 2, Table 3). A more diverse range of taxa were observed from West Hammar Marshes (L2, Figure 3, Table 3) - 3 marine, 4 brackish, 9 freshwater and 2 terrestrial taxa.

The sequence from Central Marshes (L1), although less abundant, shows a clear transition from the base to the upper part, allowing it to be split into two zones. Zone 1 falls below 250 cm. In this zone, shell material is very abundant and characterised by marine species such as *Lissotesta turritis, Tindaria virens, Abra prismatica* and *Pyrgulina* sp. There is some indication in the habitat preferences of *Abra prismatica* and *Tindaria virens* that the substrate in the marine environment was muddy. Freshwater species are also present in this zone in lower abundance, comprising *Corbicula fluminalis, Melanoides tuberculata* and *Bulinus truncatus*. Of these, only *Melanoides tuberculata* can tolerate brackish water. Whilst usually found in low salinity environments (0.2-3 ‰), it can tolerate salinity ca. 23 ‰ (Plaziat and Younis, 2005). This taxa could have been living in the same location as the marine taxa because of this tolerance, burying itself in soft sediment. Alternatively, empty shells of this species are reported to float easily (Plaziat and Younis, 2005), so they may have been transported downstream into a marine setting. There is no other evidence of brackish conditions in this zone. Both *Corbicula fluminalis* and *Bulinus truncatus* are exclusively freshwater species and seem likely to have been transported into this assemblage. *Corbicula fluminalis* is very common in modern southern Mesopotamia on fluvial channels to marshes, in a wide range of energy environments, as is *Bulinus truncatus*, also buried in soft sediments at the base of the channel (Plaziat and Younis, 2005). *Corbicula fluminalis* shells are fragile and cannot be transported far away. This suggests that exclusively freshwater environments were located close to the position of this sequence during deposition. Overall, the assemblage from Zone 1 suggests an open coastline with a very limited estuarine zone before transition to exclusively freshwater environments. The transition between marine and freshwater seems likely to have been at most only a few km north of this location.

Zone 2 is observed above 150 cm (150 to 250 cm depth is barren) and characterized by brackish and freshwater taxa only, with the exception of *Cerithidium* sp. Although *Cerithidium* sp. prefers high salinities (40-50 ‰), it can tolerate much lower salinities (1.5 ‰) if these waters are directly connected with the sea (e.g. estuarine mudflats rather than the intertidal zone). *Melanoides tuberculata* and *Bulinus truncatus* are the only taxa in common between the two zones, suggesting both freshwater (*Bulinus truncatus*) and brackish (*Melanoides tuberculata*) conditions. *Cerithidium*

sp. and *Melanoides tuberculata* both suggest a soft muddy substrate (Plaziat and Younis, 2005). Other freshwater taxa recorded in significant numbers are *Gyraulus intermixtus* and *Lymnaea radix*. These taxa are both commonly found in lacustrine environments (Plaziat and Younis, 2005) but not fluvial ones. *Gyraulus intermixtus* is more likely to be *in situ* than *Lymnaea radix* because it is found attached to subaqueous vegetation, whereas *Lymnaea radix* floats and transports readily (Plaziat and Younis, 2005). Overall, this assemblage suggests that during Zone 2, conditions at Location 1 in the Central Marshes were very similar to those at the present day (freshwater marsh and lake), but with occasional connections to an adjacent estuarine system.

In contrast, the sequence from West Hammar Marshes (L2) shows no clear succession, therefore the assemblages from all the samples are described together. The reversal of the radiocarbon ages from this sequence (section 3.2) suggests that there may have been reworking of these sediments. All three marine taxa from this sequence are found in coastal environments and in the case of *Cerithidium*, often on tidal flats in estuaries (Plaziat and Younis, 2005). They are therefore consistent with preservation within an estuarine environment. An estuarine interpretation is also possible on the basis of the four brackish taxa (Figure 3), although *Theodoxus jordani* is also found in freshwater lakes and marshes, as are *Melanoides tuberculata* and *Melanopsis praemorsum* (Plaziat and Younis, 2005). The *Melanopsis praemorsum* found here (Figure 4: 18) is a more nodular form characteristic of freshwater, so may indicate that a freshwater lake with some estuarine inputs is a more likely environment. Slow or standing water is also indicated by the *Gyraulus* sp., *Bulinus truncatus* and *Lymnaea natalensis* present in the sequence (Plaziat and Younis, 2005). *Corbicula fluminalis*, whilst dominant in fluvial channels in this region, is also found in more mixed assemblages in lakes and marshes.

The presence of two terrestrial snails (Hygromidae and *Sphinterochila baetica*) suggests proximity to dry land because transport of such species will be over short distances only. Overall, therefore, the environment during deposition of the sequence at West Hammar Marsh (L2) from ca. 2500 to 1600 BP (Table 2) seems to have been a freshwater lake or marsh with drier land nearby and occasional estuarine inputs. This suggests a rapid period of regression from the shoreline position near Central Marsh (L1) at ca. 3500 to 2800 BP to considerably further south of location 2 in West Hammar Marshes, which appears to be largely freshwater only 1000 or less years later. At the present day, the tidal limit of both Tigris and Euphrates is at Qurna, at the head of the Shatt Al Arab. However, naturally it would be further inland because there is now a tidal barrier in place.

Our results suggest therefore that the current landscape configuration, at least north of Qurna, was largely in place by the time of deposition of the West Hammar Marsh sequence. This rapid change in environments fits well with the reconstruction of the Naval Intelligence Division (1944) who suggest the formation of a lagoon at this time after progradation of the Karun delta blocked direct access to the marine waters of the Arabo-Persian Gulf. Heyvaert and Baeteman (2007) show on the basis of multiple radiocarbon dated sequences in southwest Iran, that the Karun delta had almost reached the Shatt-al-Arab by ca. 2500 BP and continued to prograde, with no evidence of tidal conditions north of Basra by 1240 BP. This evidence further backs up our interpretation.

4. Discussion

As noted in section 1.1, the position of the Arabo-Persian Gulf shoreline after the maximum marine transgression at ca. 6000 BP is much debated. Our sedimentary cores date from the later part of this post-trangression phase, when the final phases of delta infilling by the Tigris and Euphrates were occurring. The present study reports molluscan analysis and radiocarbon dating of shells from two locations in both Central (L1) and West Hammar (L2) Marshes (Figure 1b). From these, we estimate the extent and timing of marine transgression and regression at the head of the Arabo-Persian Gulf. The L1 sequence from Central Marsh shows a clear transition from marine to freshwater conditions,

separated by a series of barren samples. The base of the sequence recovered dates from ca. 5500 to 5000 cal. BP, a time when all published reconstructions place the shoreline north of this location. The base of the sequence contains mostly marine taxa with some freshwater taxa, suggesting that although there must have been some transport of shells from upstream, the shoreline remained near to Central Marsh throughout this time, up till the top of the zone, which has been estimated to date from approximately 3500 to 2800 cal. BP using a simple linear age-depth relationship. This conflicts with the shoreline reconstruction of Aqrawi (2001), who stated that regression was complete by this date. It is very similar to the estimated shoreline position suggested by the Naval Intelligence Division and slightly further north than suggested by Hritz et al. (2012b) (Table 1). The upper part of the sequence at Central Marsh (L1) shows a transition to freshwater marsh with limited terrestrial influence, as it is at the present day, being upstream of the tidal limit at Qurna. The exact dating of this part of the sequence is unclear due to insufficient shell material for radiocarbon age determinations. The sequence from L2 in West Hammar Marsh dates from a later period (ca. 2500 to 1600 cal. BP). This sequence is further south (Figure 1b) and does not show a clear succession, most likely because of reworking of sediments, but gives a broad picture of inputs from marine, freshwater and even terrestrial environments. At present this core is located close to the main channel of the Euphrates and was likely within the former floodplain of this river. If the tidal limit of the river was only slightly further north than it is at the present day one can imagine a similar range of taxa being deposited within a dynamic fluvio-deltaic system. Thus, it seems likely that at ca. 2500-1600 BP, the shoreline was significantly further south than the West Hammar Marshes, but that this location (L2) may have been near to the tidal limit. This agrees with all previously published reconstructions. However, the rapid regression from the time of deposition of the Location 1 and 2 sequences fits best with rapid westerly progradation of the Karun delta tracked by Heyvaert and Baeteman (2007) and also suggested by the Naval Intelligence Division (1944) who reconstructed an inland lagoon between 3000 and 2000 BP north of Basra.

This finding has two main implications. Firstly, it suggests that the simple calculations of delta progradation based on assuming similar rates of sediment delivery over time from 6000 BP up to the present day provide a very good first approximation of the Arabo-Persian Gulf shoreline position at various times in the Holocene (Naval Intelligence Division, 1944). If this is true, the mountainous regions in the headwaters of the Tigris and Euphrates probably experienced very little climatic variability during the last 6000 years, delivering sediment to Mesopotamia at a similar rate throughout to that measured in 1944. Palaeoclimate records from pollen and oxygen isotopes from Lake Van in the Taurus Mountains of eastern Turkey (e.g. Wick et al., 2003) and Lake Zeribar in the Zagros Mountains in Iran (e.g. Stevens et al., 2001) shed light on the likelihood of this limited climatic variability since 6000 BP. Both records suggest that the climate of the region was broadly similar to the present day by ca. 4500 BP. In contrast, the time period from ca. 6000 to 4000 BP may have been wetter. In the Lake Van record, this is based on the late establishment of oak woodland (Wick et al., 2003), assuming that this is controlled by aridity and therefore it's establishment in 6000 BP is a sign of wetter climates. In Lake Zeribar this is based on isotopic data (Stevens et al., 2001), although the interpretation of the isotopic data has been challenged by some (e.g. Jones and Roberts, 2008; Matthews et al., 2013). If the period from ca. 6000 to 4000 BP was wetter, this could have affected sediment supply by increasing run-off and sediment delivery from the hillslopes. Alternatively, increased vegetation cover could have stabilised slopes and offset the erosive effect of any increased run-off. In summary, these palaeoclimatic records from the Tigris and Euphrates headwaters show that the climate driving sediment supply was almost certainly similar for at least 4500 years. It is possible that the climate was wetter between 4500 and 6000 BP, but not clear from this evidence if this would have affected sediment supply.

Secondly, in contrast to this relative stability in the mountainous headwaters, it has been argued that the reason for the decline of the Sumerian civilisation ca. 3000 BP related to a combination of local aridification on the Mesopotamian plain and marine regression (Kennett and Kennett, 2006; Hritz et

al., 2012). In this conceptual model, as the coastline migrated south, the valuable range of environments that populations were able to exploit would have decreased. Instead of irrigated arable land, marshland and coast, these communities are presumed to have become increasingly reliant on irrigation systems. Over time, the cost involved in producing all food in this way, and the environmental implications of long term irrigation then led to decline. Our findings suggest that the coastline was actually closer to the Sumerian cities at 3000 BP than this model of combined regression and aridification driving decline requires. Thus there may have been other reasons for the decline of the civilisation, or aridification might have been more significant in the absence of coastline retreat.

To assess the significance of aridification it is necessary to investigate palaeoclimate records from adjacent regions. There is a widespread aridification event reported from 4200 BP that has been linked with the collapse of the Old Kingdom in Egypt, the Early Bronze Age civilisations of Greece and Crete, and the Akkadian Empire in Mesopotamia (Dixit et al., 2014). This aridification is seen very clearly in the Lake Zeribar record from Iran (Stevens et al., 2001) between 4-3500 BP and sustained from 4200 BP to the present day in Lake Van in Turkey (Wick et al., 2003). In Mesopotamia itself, the floods found at Ur, Kish, Fara and Nineveh between 5500 and 4400 BP may suggest a reduction in rainfall at a similar time to this event (Ellison, 1978). There is also evidence for a slight increase in aridity around 3000 BP from Jeita Cave, Lebanon (Verheyden et al., 2008), following a wetter period from 4-3000 BP. This is later than seen at Lake Zeribar (Stevens et al., 2001). In the absence of a consistent signal from long palaeoclimatic records from the Mesopotamian plain, useful information can be gained by looking at adjacent marine records such as core M5-422 in the Gulf of Oman, downwind of Mesopotamia (e.g. Cullen et al., 2000). Here, mineralogic and geochemical analyses of Neodynium and Strontium document a very abrupt increase in eolian dust which is interpreted to represent Mesopotamian aridity, radiocarbon dated to 4025 ± 125 cal. BP and persisting for ca. 300 years. There is also evidence of mean SSTs that were warmer than at present (ca. 1.3 °C ± 0.3 °C) at ca. 4300 BP further east in the Indian Ocean (Abram et al., 2009).

Therefore there is some agreement between records that climate generally became more arid at some point after 4000 BP, although there is no terrestrial Mesopotamian record that conclusively demonstrates the timing of this. As discussed above, the particular time period of interest in this study is the end of the Sumerian period ca. 3000 BP. If marine regression at this time was less than previously thought, as suggested by our records, aridification may have been more significant in dictating the end of this civilization. However, more local palaeoclimatic evidence is needed to assess the case for the extent and exact timing of aridification that may have driven archaeological change at the end of the Sumerian period.

5. Conclusions

This study reports two radiocarbon dated molluscan sequences from the West Hammar and Central Marshes in southern Iraq. In Central Marsh these show a marine assemblage below ca. 3500 to 2800 cal. BP, transitioning to a freshwater / brackish assemblage after this time. From West Hammar Marsh we report a mixed estuarine / freshwater / terrestrial assemblage from a more southerly sequence dated to ca. 2500 to 1600 cal. BP. This suggests that the coastline was further north than previously suggested at ca. 3000 BP and then rapidly regressed. Our sedimentary sequences provide a similar reconstruction to that suggested by the Naval Intelligence Division (1944) and agree with recent work on the Karun delta (Heyvaert and Baetman, 2007). The former reconstruction is based on assumed similar rates of sediment delivery throughout the post-6000 BP period since the maximum marine trangression. This suggests that the rates of sediment delivery to the Tigris-Euphrates delta have not changed naturally during this time. Whilst there were some climatic

changes over this time period in the headwater regions of the Tigris and Euphrates, it is plausible that they did not affect the sediment supply due to increased vegetation stabilization of hillslopes.

Our research also has implications for the reasons given for the ending of the Sumerian civilisation ca. 3000 BP. If the marine regression occurred later than some authors (e.g. Aqrawi, 2001; Hritz et al., 2012b) suggested, then aridification might have been a more significant driver of change than previously thought because marine resources were still available to these communities. There is, however, no consistent evidence of this aridification at a specific time in local records. Marine archives from the Arabo-Persian Gulf have the potential to address this issue because they provide continuous palaeoclimatic records including dust fluxes from Mesopotamia (Cullen et al., 2000) that suggest an increase in aridity around 4200 BP. Ongoing work analyzing ostracods and foraminifera from these sequences should also shed further light on some of these issues.

Acknowledgements

IA would like to express grateful thanks to Department of Geography and Department of Earth and Planetary Sciences, Birkbeck, University of London for their generous hospitality during his year in London and the Iraqi Government for their funding of this. We also express sincere thanks for help with identification of taxa to Professor David Horne, School of Geography, Queen Mary, University of London and Dr Andreia Salvador, Curator of Marine Mollusca, Department of Life Sciences, Natural History Museum, London.

References

Abram N.J., McGregor H.V., Gagan M.K., Hantoro W.S., Suwargadi B.W., 2009. Oscillations in the southern extent of the Indo-Pacific Warm Pool during the mid-Holocene. *Quaternary Science Reviews* 28, 2794-2803.

Ainis, A., Vellanoweth R., Lapena Q., Thornber CA., 2014. Using non-dietary gastropods in coastal shell middens to infer kelp and seagrass harvesting and paleoenvironmental conditions. *Journal of Archaeological Science* 49, 343-360. doi.org/10.1016/j.jas.2014.05.024.

Al-Jiburi H.K., Al-Basrawi, N.H., 2011. Hydrogeology of the Mesopotamia Plain. *Iraqi Bulletin of Geology and Mining* Special Issue 4, 83-103.

Alves, E.Q., Macario, K., Ascough, P., Ramsey, C.B., 2018. The worldwide Marine Reservoir Effect: definitions, mechanisms, and prospects. *Reviews of Geophysics* 56, 278-305.

Aqrawi, A.A. 2001. Stratigraphic signatures of climatic change during the Holocene evolution of the Tigris–Euphrates delta, lower Mesopotamia. *Global and Planetary Change* 28, 267-283.

Ascough, P., Cook, G., Dugmore, A., 2005. Methodological approaches to determining the marine radiocarbon reservoir effect. *Progress in Physical Geography*, 29, 532-547.

Baqer, T., 1980. *Introduction to the history of ancient civilisations*. First edition, Alwarrak Publishing Ltd, P.31.

Broecker, W.S., Cember, R.P., Toggweiler, J.R., Trombore, S.E., White, J., 1987. Final report on the

Lamont-Doherty geological observatory coral radioisotope project. DOE/EV/10041C-1 (unpublished).

Bronk Ramsay, C., 2009. Bayesian analysis of radiocarbon dates. *Radiocarbon* 51, 337-360.

Clarke, J., Brooks, N., Banning, E., Matthews, M., Campbell, S., Clare, L., Cremaschi, M., Lernia, S., Drake, N., Gallinaro, M., Manning, S., Nicoll, K., Philip, G., Rosen, S., Schoop, U., Tafuri, M., Weninger, B., Zerboni, A., 2016. Climatic changes and social transformations in the Near East and North Africa during the 'long' 4th millennium BC: A comparative study of environmental and archaeological evidence, *Quaternary Science Reviews* 136, 96-121, doi.org/10.1016/j.quascirev.2015.10.003.

Cooke, G.A., 1987. Reconstruction of the Holocene coastline of Mesopotamia. *Geoarchaeology* 2, 15-28.

Cullen, H.M., deMenocal, P.B., Hemming, S., Hemming, G., Brown, F.H., Guilderson, T., Sirocko, F., 2000. Climate change and the collapse of the Akkadian empire: Evidence from the deep sea. *Geology* 28, 379–382.

Dixit, Y., Hodell D.A., Petrie CA.A., 2014. Abrupt weakening of the summer monsoon in northwest India ~4100 yr ago. *Geology* 42, 339-342.

Dunbar, E., Cook, G.T., Naysmith, P., Tripney, B.G., Xu, S., 2016. AMS 14C dating at the Scottish Universities Environmental Research Centre (SUERC) radiocarbon dating laboratory. *Radiocarbon* 58(1), pp.9-23.

Ellison, E.R., 1978. *A study of diet in Mesopotamia (ca.3000 - 600 BC) and associated agricultural techniques and methods of food preparation*. Doctor of Philosophy, Faculty of Arts, University of London, P. 10.

Heyvaert, V.M.A., Baeteman, CA., 2007. Holocene sedimentary evolution and palaeocoastlines of the Lower Khuzestan plain (southwest Iran). *Marine Geology*, 242, 83-108.

Hritz, CA., Pournelle, J., Smith, J., Albadran, B., Issa, B.M., Al-Handal, A., 2012a. Mid-Holocene dates for organic-rich sediment, palustrine shell, and charcoal from southern Iraq. *Radiocarbon* 54, 65-79.

Hritz, CA., Pournelle, J., Smith, J., 2012b. Revisiting the sealands: report of preliminary reconnaissance in the Hammar District, Dhi Qar and Basra governates, Iraq. *Iraq* 74, 37-49.

Jassim, S.Z., Goff J.CA., 2006. *Geology of Iraq*. Dolin, Czech Republic, P.192.

Jones, M.D., Roberts, CA.N., 2008. Interpreting lake isotope records of Holocene environmental change in the Eastern Mediterranean. *Quaternary International* 181, 32-38.

Kennett, D.J., Kennett, J., 2006. Early State Formation in Southern Mesopotamia: Sea Levels, Shorelines, and Climate Change. *Journal of Island and Coastal Archaeology* 1, 67–99, DOI:10.1080/15564890600586283.

Langejans G., Dusseldorp G., Thackeray, J. 2017. Pleistocene molluscs from Klasies River (South Africa): Reconstructing the local coastal environment. *Quaternary International* 427, 59-84. doi.org/10.1016/j.quaint.2016.01.013.

Matthews, W., Mohammadifar, Y., Motarjem, A., Ilkhani, H., Shillito, L.M., Matthews, R., 2013. Issues

in the study of palaeoclimate and palaeoenvironment in the early Holocene of the central Zagros, Iran. *International Journal of Archaeology* 1, 26-33.

Naval Intelligence Division, 1944. *Iraq and the Persian Gulf.* Geographical Handbook Series B.R. 524. London: British Admiralty.

Plaziat, J.CA., Younis, W.R., 2005. The modern environments of Molluscs in southern Mesopotamia, Iraq: A guide to paleogeographical reconstructions of Quaternary fluvial, palustrine and marine deposits. *Carnets de Géologie/Notebooks on Geology*, Brest, Article, 1.

Reimer, P.J., Bard, E., Bayliss, A., Beck, J.W., Blackwell, P.G., Ramsey, CA.B., Buck, CA.E., Cheng, H., Edwards, R.L., Friedrich, M., Grootes, P.M., 2013. IntCal13 and Marine13 radiocarbon age calibration curves 0–50,000 years cal BP. *Radiocarbon* 55, 1869-1887.

Reimer, R.W., Reimer, P.J., 2016. An online application for ΔR calculation. *Radiocarbon* 13, 1-5.

Sanlaville, P. 1989. Considération sur l'évolution de la basse Mésopotamie au cours des derniers milléniares. *Paléorient* 15, 5-27.

Sharland, P.R., Archer, R., Casey, D. Davies, R.H., Simmons, MD, 2001. Arabian plate sequence stratigraphy. *GeoArabia Special Publication* 2, p.371.

Southon, J., Kashgarian, M., Fontugne, M., Metivier, B., Yim, W. W-S., 2002. Marine reservoir corrections for the Indian Ocean and southeast Asia. *Radiocarbon* 44, 167-180.

Stevens, L.R., Wright Jr, H.E., Ito, E., 2001. Proposed changes in seasonality of climate during the Lateglacial and Holocene at Lake Zeribar, Iran. *The Holocene* 11, 747-755.

UNEP (2001). *The Mesopotamian Marshlands: Demise of an Ecosystem*, Division of Early Warning and Assessment, United Nations Environment Programme, Nairobi, Kenya.

Ur, J., 2012. *A Companion to the Archaeology of the Ancient Near East*. Edited by D.T. Potts., Blackwell Publishing Ltd., P. 535.

Ur, J., 2014. Households and the Emergence of Cities in Ancient Mesopotamia. *Cambridge Archaeological Journal* 24, 249–268. doi:10.1017/s095977431400047x.

Verheyden, S., Nader, F.H., Cheng, H.J., Edwards, L.R., Swennen, R., 2008. Paleoclimate reconstruction in the Levant region from the geochemistry of a Holocene stalagmite from the Jeita cave, Lebanon. *Quaternary Research* 70, 368-381.

Wick, L., Lemcke, G., Sturm, M., 2003. Evidence of Lateglacial and Holocene climatic change and human impact in eastern Anatolia: high-resolution pollen, charcoal, isotopic and geochemical records from the laminated sediments of Lake Van, Turkey. *The Holocene* 13, 665-675.

Radiocarbon years BP	Calendar years BC	Archaeological period	Historical period	Shoreline location based on sediment analysis and radiocarbon dating from boreholes (Aqrawi, 2001)	Shoreline position based on archaeological data and delta modelling (Naval Intelligence Division, 1944)	Shoreline based on radiocarbon-dated sedimentary sequences (Hritz et al., 2012a,b)*
8000-6000		'Ubaid		Transgression		
6000-5000	4000-3000	Chalcolithic / Uruk		Shoreline near Nasiriya		6000 – 4000 BP Shoreline north of Hammar Marsh
5000-3000	3000-1000	Bronze Age	Sumerian	Gradual regression	5000 BP Shoreline north of Ur	
					4000 BP Shoreline from Ur to Amara	
3000-present	1000-490	Iron Age	Assyrian / Babylonian / Kassite / Assyrian	3000 BP Shoreline at present-day position	3000 BP Shoreline south of Ur, north of Qurna	c. 3000 BP Shoreline at Basra
	550		Persian		2000 BP Shoreline south of Basra	c. 2000 BP Shoreline south of Basra
	490	Classical Antiquity	Hellenistic		1000 BP Shoreline at present day position	

Table 1 Archaeological chronology for southern Mesopotamia with approximate radiocarbon and calendar years after Kennett and Kennett (2006) and Ur (2012). Different published shoreline positions are shown. *Radiocarbon dates are presented in Hritz et al., 2012a and the shoreline reconstruction in Hritz et al., 2012b. Most of the published radiocarbon dates are from the Early Holocene marine transgression, meaning that the later period (ca. 5000 to 1000 BP) is based on fewer radiocarbon-dated tie-points.

Laboratory number	Sequence	Depth (cm)	Species dated	Calibration curve	MRE	Age (^{14}C yr BP)	Calibrated age ranges (cal. BP)
Estimated by age-depth model	Central Marsh (L1)	230	N/A	IntCal13	N/A	2989 ± 149 (est.)	3480-2786 (95.4%)
SUERC-74783 (GU44752)	Central Marsh (L1)	320	*Corbicula fluminalis*	IntCal13	N/A	4159 ± 29	4828-4781 (19.0%) 4770-4581 (76.4%)
SUERC-74784 (GU44753)	Central Marsh (L1)	500	*Corbicula fluminalis*	IntCal13	N/A	4578 ± 29	5445-5410 (12.2%) 5325-5275 (55.4%) 5177-5175 (0.1%) 5169-5122 (15.1%) 5110-5067 (12.5%)
SUERC-74778 (GU44750)	Hammar Marsh (L2)	180	*Melanoides tuberculata*	Marine13	0 ± 50	2633 ± 29	2484-2313 (68.2%) 2552-2209 (95.4%)
				Marine13	180 ± 53		2416-2206 (95.4%)
SUERC-74779 (GU44751)	Hammar Marsh (L2)	360	*Melanopsis praemorsum*	Marine13	0 ± 50	2111 ± 29	1838-1679 (68.2%) 1902-1612 (95.4%)
				Marine13	180 ± 53		1796-1596 (95.4%)

Table 2. Radiocarbon age estimates from sequences reported in the paper. Calibration was undertaken using OxCal 4 (Bronk-Ramsay, 2009) and the calibration curves IntCal13 and Marine13 (Reimer et al., 2013), with a Marine Reservoir Effect (MRE) from the Marine Reservoir Database (Reimer and Reimer, 2016).

Species	Habitat	Location	Family-level taxa			
			Class	Order	family	Genus
Dikoleps templadoi	Marine	L1	Gastropoda	Archaeogastropoda	Turbinidae	Dikoleps (Dantart and Luque, 2004)
Abra prismatica	Marine	L1	Bivalvia	Veneroida	Semelidae	Abra (Montagu, 1808)
Pyrgulina Sp.	Marine	L1+L2	Gastropoda	Odostomiinae	Pyramidellidae	Chrysallida (Adams, 1864)
Lissotesta turrita	Marine	L1	Gastropoda	Seguenzioidea	Seguenzioidea	Lissotesta (Iredale, 1915)
Tindaria virens	Marine/coastal	L1+L2	Bivalvia	Nuculoida	Nuculanidae	Tindaria (Dall, 1890)
Cerithidium	Marine/brackish	L1+L2	Gastropoda	Neotaenioglossa	Cerithiidae	Cerithidium (Monterosato, 1884)
Puperita pupa	Brackish/freshwater	L2	Gastropoda	Neritopsina	Neritidae	Puperita (Linnaeus, 1767)
Melanoides tuberculata	Freshwater/brackish	L1+L2	Gastropoda	Architaenioglossa	Thiaridae	Pomacea (Müller, 1774)
Melanopsis praemorsum	Freshwater/brackish	L2	Gastropoda	Clade	Melanopsidae	Melanopsis (Linnaeus, 1758)
Theodoxus jordani	Freshwater/brackish	L2	Gastropoda	Cycloneritimorpha	Neritidae	Theodoxus (P.D. Montfort, 1810)
Gyraulus intermixtus	Freshwater	L1+L2	Gastropoda	Clade*	Anisus	Planorbis (Mousson, 1894)
Gyraulus acronicus	Freshwater	L2	Gastropoda	Basommatophora	Planorbidae	Gyraulus (Acronicus A. Ferussac, 1807)
Gyraulus Sp.	Freshwater	L1+L2	Gastropoda	Basommatophora	Planorbidae	Gyraulus (Agassiz, 1837)
Bulinus truncatus	Freshwater	L1+L2	Gastropoda	Bulinini	Planorbidae	Bulinus (Audouin, 1827)
Lymnaea Radix	Freshwater	L1	Gastropoda	Hygrophila	Lymnaeidae	Lymnaea (Peregra Mull)
Lymnaea natalensis	Freshwater	L2	Gastropoda	Basommatophora	Lymnaeidae	Lymnaea (Krauss, 1848)
Theodoxus anatolicus	Freshwater	L2	Gastropoda	Neritopsina	Neritidae	Theodoxus (Recluz, 1841)
Valvata	Freshwater	L2	Gastropoda	Heterostropha	Valvatidae	Valvata (Müller, 1774)
Corbicula fluminalis	Freshwater	L1+L2	Bivalvia	Vererida	Cyrenidae	Corbicula (Müller, 1774)
Sphaerium	Freshwater	L2	Bivalvia	Veneroida	Pisidiidae	Sphaerium (Scopoli, 1777)
Hygromiidae	Terrestrial	L2	Gastropoda	Stylommatophora	Hygromiidae	(Tryon, 1866)
Sphincterochila baetica	Terrestrial	L2	Gastropoda	Stylommatophora	Sphincterochila	Sphincterochila (Rlossmassler, 1854)

Table 3: Marine, Non-Marine and Terrestrial molluscs recorded from Locations 1 and 2 (L1, L2). Clade* a group of organisms believed to have evolved from a common ancestor, according to the principles of cladistics.

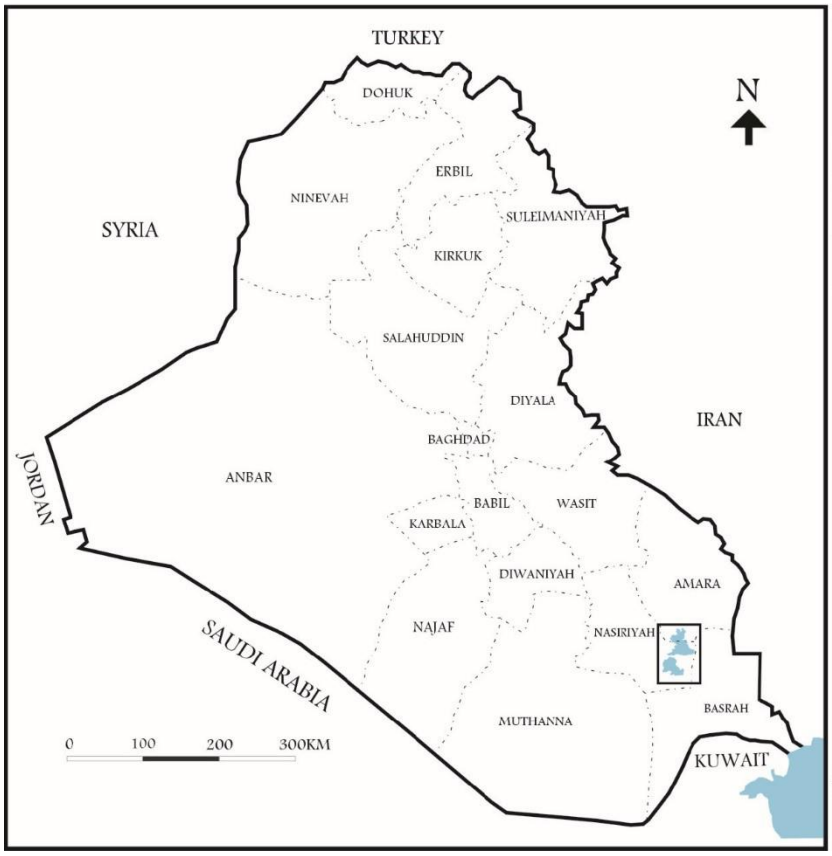

Figure 1a. Location of study area within southern Iraq.

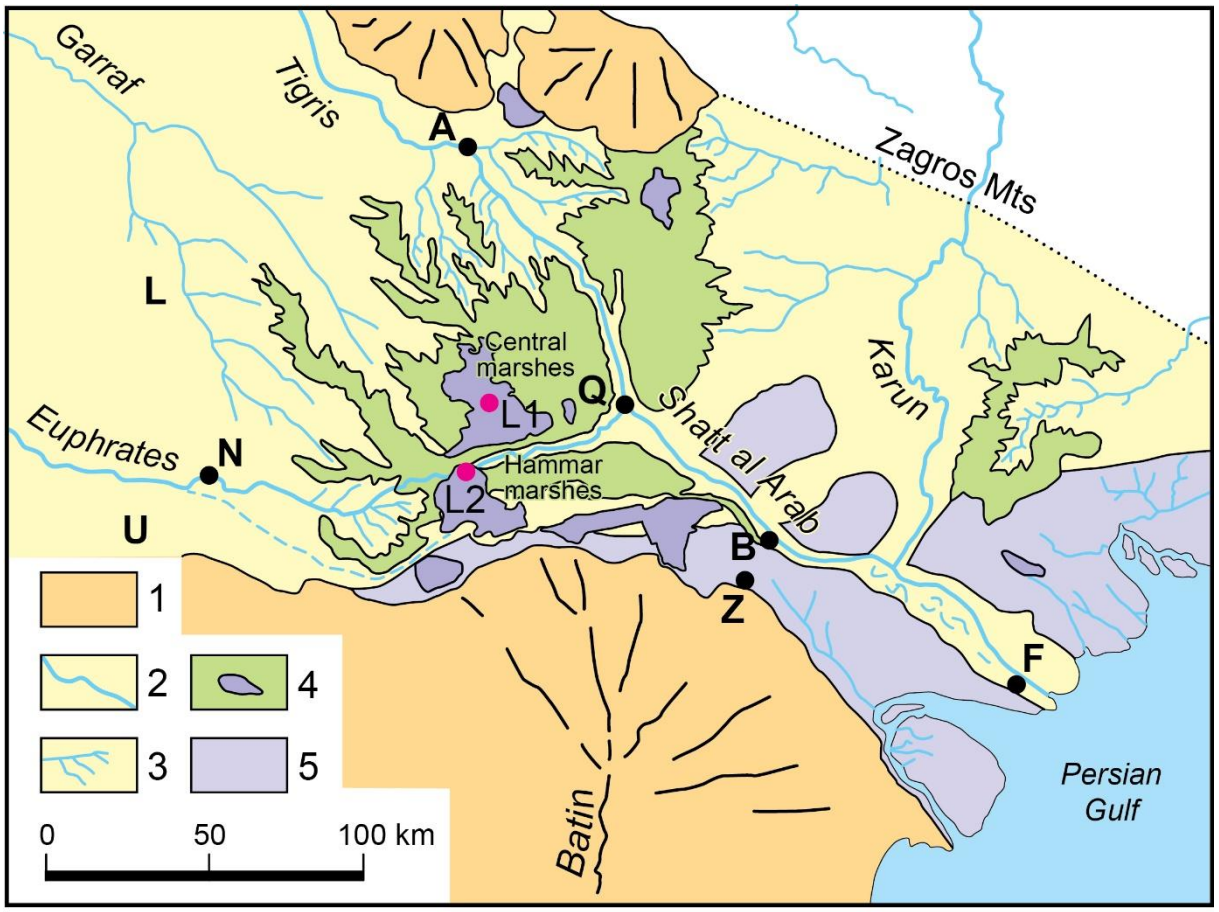

Figure 1b. Exact location of sedimentary cores in the Central (L1) and West Hammar (L2) Marshes, showing major morphosedimentary units in the region after Plaziat and Younis (2005). 1 = alluvial fans, 2 = fluvial channel and levees, 3 = lacustrine delta, 4 = marsh and lake, 5 = sabkha. Locations added to aid readers in placing the sequences studied in context: A = Amara, B = Basra, F = Fao, N = Nasiriya, Q = Qurna, Z = Zubair, L = Lagash, U = Ur.

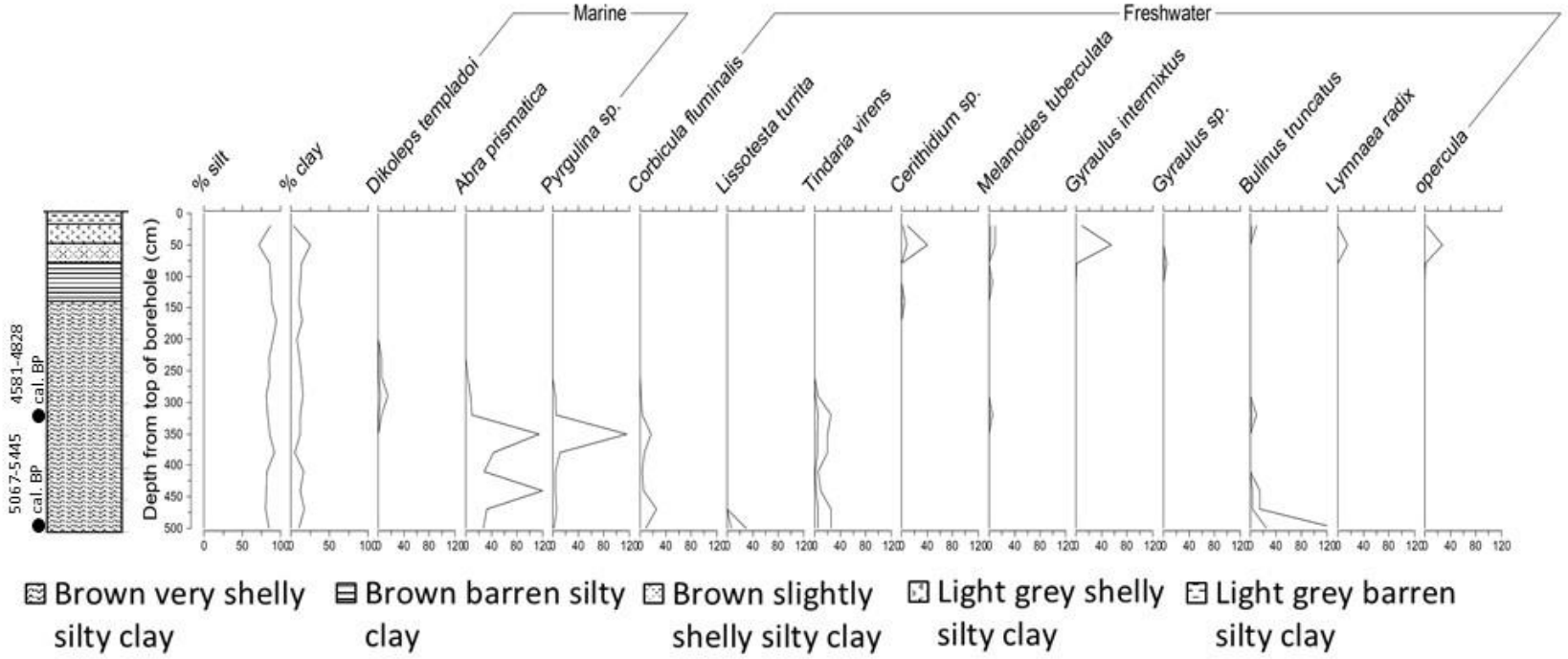

Figure 2: Sediment sequence, radiocarbon ages and mollusc assemblages from Central Marshes (L1).

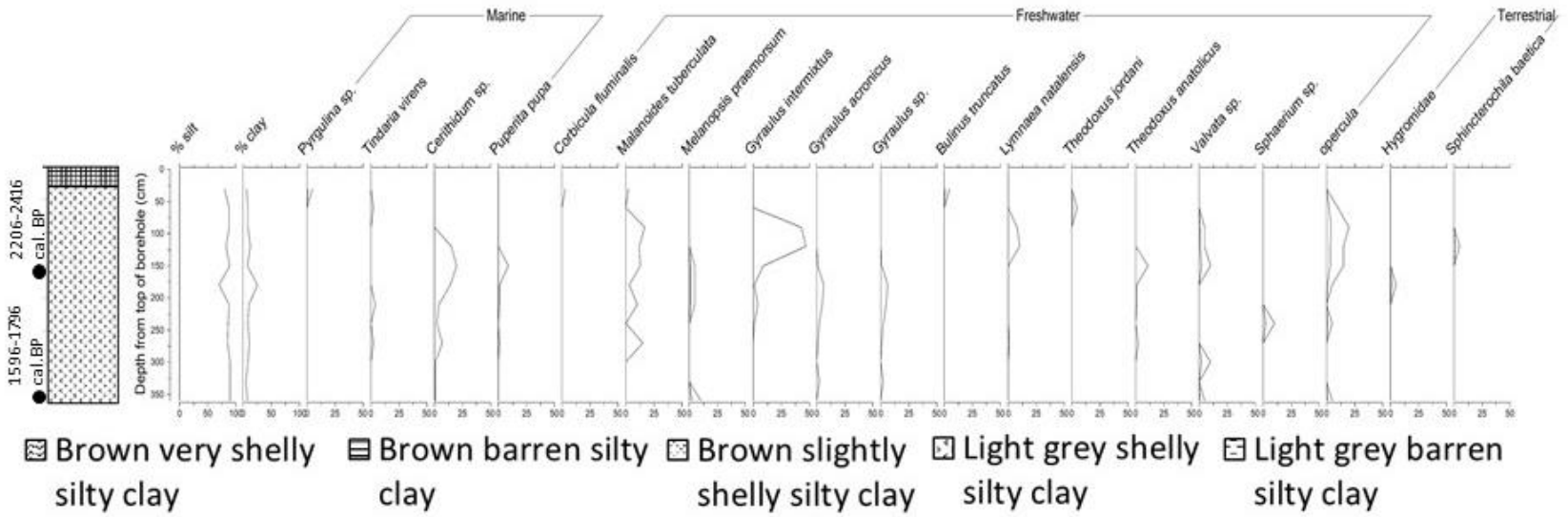

Figure 3: Sediment sequence, radiocarbon ages and mollusc assemblages from West Hammar Marsh (L2).

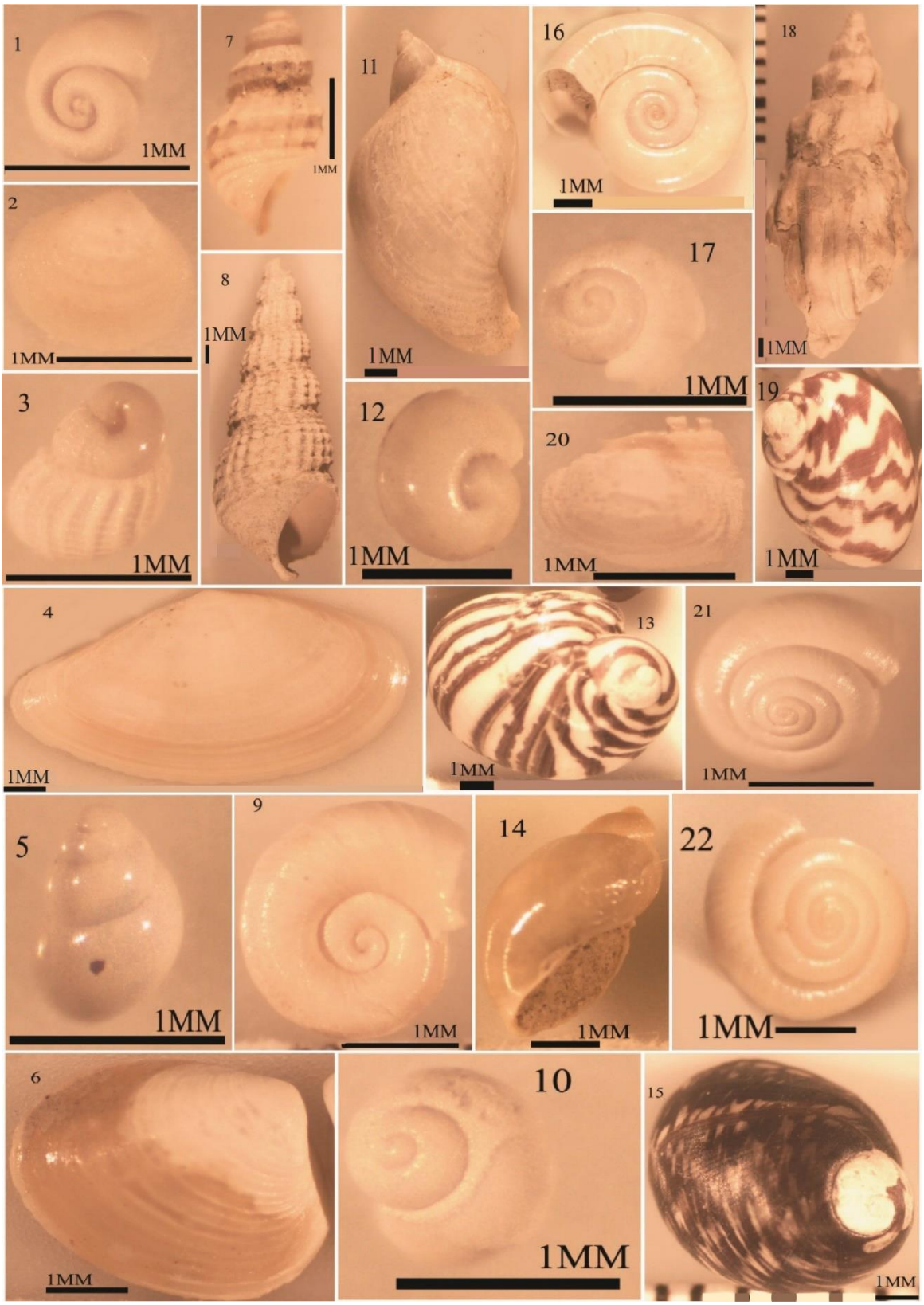

Figure 4: Marine, Non Marine and Terrestrial (Gastropoda, Bivalvia) from L1, L2: *1.Dikoleps templadoi, 2. Abra prismatica, 3.Pyrgulina Sp., 4.Corbicula fluminalis, 5. Lissotesta turrita, 6.Tindaria virens, 7.Cerithidium, 8.Melanoides tuberculata, 9.Gyraulus intermixtus, 10.Bulinus truncates, 11.Lymnaea Radix, 12.Gyraulus Sp., 13.Puperita pupa, 14.Lymnaea natalensis, 15.Theodoxus jordani, 16.Gyraulus acronicus, 17.Valvata, 18. Melanopsis praemorsum, 19. Theodoxus anatolicus, 20.Sphaerium, 21.Hygromiidae, 22.Sphincterochila baetica.*

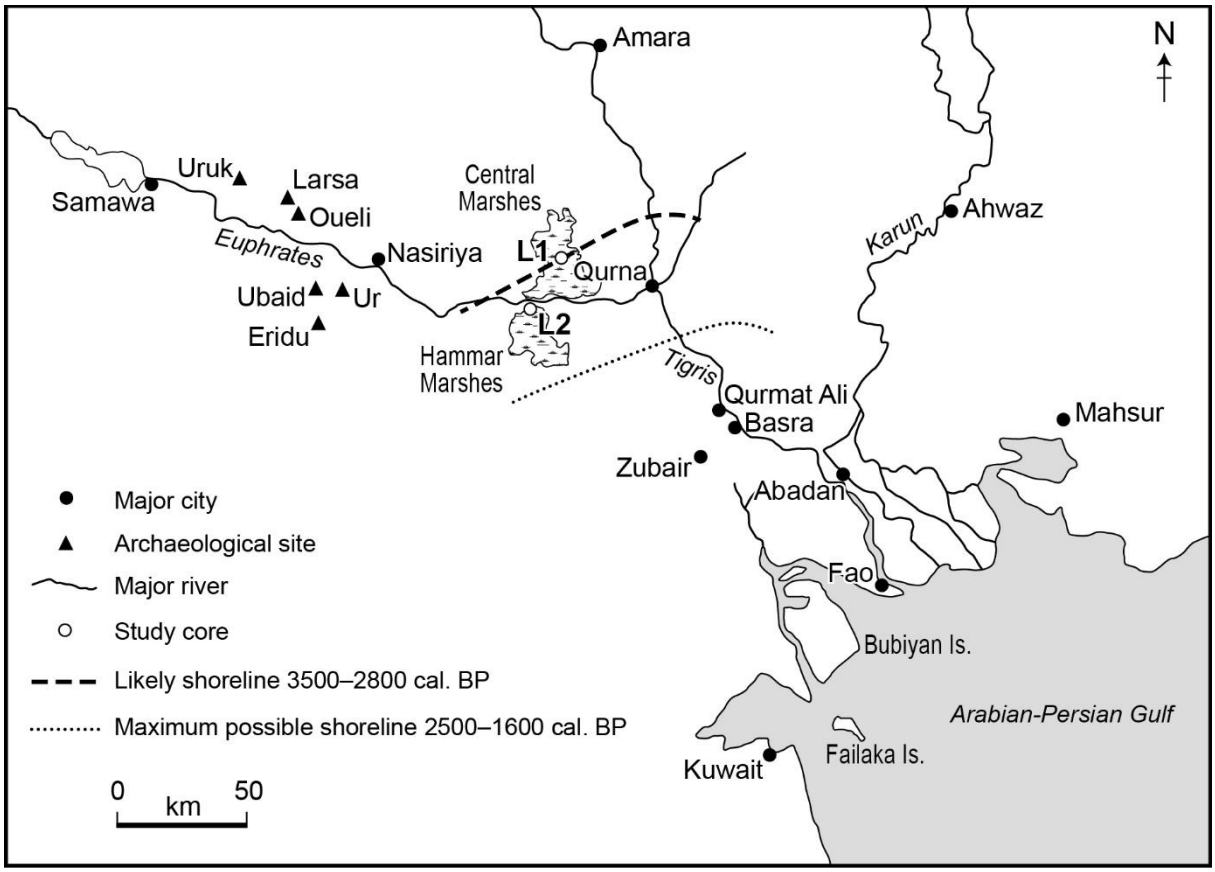

Figure 5. Reconstructed shorelines from mollusc sequences from Central and West Hammar Marshes (Locations 1 and 2).